Asian Journal of Chemistry; Vol. 28, No. 5 (2016), 987-992

ASIAN JOURNAL OF CHEMISTRY

http://dx.doi.org/10.14233/ajchem.2016.19558

Study of Glucose Adsorption on Synthetic Humin

A. WAHYUNINGTYAS*, R. ROTO and A. KUNCAKA

Department of Chemistry, Universitas Gadjah Mada, Yogyakarta 55281, Indonesia

*Corresponding author: E-mail: aultyas@gmail.com

Received: 10 August 2015; *Accepted*: 30 October 2015; *Published online*: 30 January 2016; AJC-17730

Synthetic humin, a new kind of adsorbents, has been synthesized and the adsorption of glucose on synthetic humin has been performed. The starting compound was obtained by leaching synthetic humus, which has been made by mixing biochar and hydrochar, by solution of 0.5 M NaOH. The effects of contact time, initial glucose concentration and pH on the adsorption process were studied through batch experiment. After adsorption, the residual glucose concentration was measured by UV-visible spectrometry using Nelson-Somogyi method. Results show that the synthetic humin can adsorp100 ppm glucose concentration completely at 48 h. Both the Langmuir and Freundlich models have analyzed the adsorption isotherm. However, the adsorption data were best fitted to the Freundlich isotherm with K value 0.00478 mg g^{-1}. The adsorption of glucose by humin follows Ho's pseudo-second order kinetic model. It was found that the adsorption capacity of humin was 4.8 mg g^{-1} with rate constant of 8.42×10^{-5} g mg^{-1} min^{-1}.

Keywords: Synthetic humin, Glucose adsorption.

INTRODUCTION

Soil organic matter (SOM) is important for soil fertility. Soil organic matter is defined as a group of carbon containing compounds originated from living things and deposited in soil. Soil organic matter contains mainly elemental carbon (55 %), nitrogen (5-6 %), phosphorous (1 %) and sulfur (1 %) [1]. A fertile soil contains at least 5 % soil organic matter. Soil organic matter itself comprises 2.5 % organic carbon and 50 % humin [1]. Today, about 2-5 % of soil organic matter decomposes annually [2] and causes the soil organic matter content in soil to reduce to be near 2 %. This will threaten the world food security where agriculture productivity decreases as a result of low soil nutrient contents needed for plants' growth. Therefore, a method to restore quickly the soil organic matter content is critical.

Combining the Terra Preta de Indio (TPI) soil concept [3] and the supramolecular humus theory [4,5], we have prepared synthetic humus that we called slow release organic paramagnetic fertilizer (SROPF). This slow release organic paramagnetic fertilizer prepared by mixing biochar and hydrochar, which was expected to be able to increase carbon content soil to help increase agriculture products. The slow release organic paramagnetic fertilizer application on agricultural soil causes the soil organic matter content in soil to increase by 0.36 % and results in doubling some agriculture products.

The increase in soil organic matter content in soil is caused by the ability of the synthetic humin to hold biomolecules produced from biomass decomposition and forms a stable interaction [6]. Carbohydrates are the largest biomolecules available in the humus [7] and can be decomposed by microbial activity to release glucose as an intermediate product. Approximately, humus consists of about 30-40 % free glucose [8], which easily converts to gaseous CO_2.

We reported here on a model of adsorption of glucose by synthetic humin. It is one of many ways to increase carbon content in soil. The glucose adsorption process on synthetic humin is evaluated by kinetics' pseudo first order and pseudo second order. The Langmuir and Freundlich models were also used to analyze the glucose adsorption equilibrium on synthetic humin.

EXPERIMENTAL

Synthetic humus was synthesized by mixing biochar from rice husk pyrolysis and hydrochar from hydrothermal carbonization of poultry manure. Granular powder of β-D-glucose, sodium hydroxide, nitrogen gas, Nelson reagents A and B, arsenomolybdate solution and distilled water. All chemicals were of reagent grade and used without further purification.

Synthetic humin characterized by IR spectrometry (Shimadzu-8201 PC FT-IR Spectrometry with KBr plat), X-ray diffraction [Shimadzu XD-3H with Cu source K_α (λ = 15406

Å) and Ni filter] and surface area analyzer (Quantachome NovaWin2). The residual glucose concentration in solution was measured using UV-visible spectrometry (Cintra), through Nelson-Somogyi method.

Procedure

Extraction of synthetic humin: The extraction and purification of synthetic humin from synthetic humus performed according to the IHSS procedure for extraction of soil humic substances [8]. Dry synthetic humus was weighed, 0.5 M NaOH (aq) by ratio 1:10 was added under nitrogen atmosphere for 10 min then shake mixture for 24 h. In order to remove the alkaline residual, the synthetic humin fraction washed with distilled water until the supernatant was colourless. The pure synthetic humin dried at 100 °C and sieved through a 100-mesh grid. Finally, the synthetic humin was characterized by FT-IR, X-ray diffraction and surface area analysis.

Adsorption studies: Study of glucose adsorptions on synthetic humin were carried out using batch equilibrium method in 100 mL glass bottle. Each test consisted of mixing a 25 mL of glucose solution and 0.5 g synthetic humin. Various initial glucose concentration were used in each batch: 10, 20, 40, 100, 200 and 300 mg L^{-1} to investigate the effect of initial glucose concentration to glucose adsorption on synthetic humin. The suspensions were shaken for 2 h at 40 μA at ambient temperature shaker. After mixing, the samples were centrifuged at 5000 rpm for 10 min and the residual glucose concentration in the solution analyzed by UV-visible spectrometry through Nelson-Somogyi method. The pH of the solution was also ranged between 4-9 to investigate the effect of pH. Finally, the adsorption experiment were carried out for various contact time of 1 h, 2 h, 3 h, 6 h, 12 h, 24 h, 48 h, 3 days, 2 weeks and a month.

The adsorption capacity at the time t, q_t (mg g^{-1}) is calculated as:

$$q_t = \frac{(C_i - C_t) \times V}{m} \quad (1)$$

where C_i and C_t represent the initial and final (at any time t) concentration (mg L^{-1}) of glucose, respectively, V is the volume of the solution and m is the mass of synthetic humin (g).

Desorption studies: Batch desorption experiment was performed exactly in the same condition with adsorption experiment, but in blank solution of adsorbate (free glucose solution).

Measurement glucose concentration by Nelson-Somogyi method: The glucose concentration in supernatant was measured by UV-visible spectrometry through Nelson-Somogyi method. This method is based on the glucose properties as reducing sugar. When reducing sugars heated with alkaline copper tartrate, copper is reducing from cupric to cuprous state and thus cuprous oxide formed. When cuprous oxide treated with arsenomolybdic acid, the molybdic acid is reducing to molybdenum blue. The blue colour developed is compared with a set of standards at λ_{max}.

Mix 1 mL of Nelson reagent B and 25 mL of Nelson reagent A before used, to form solution C. Then, 1 mL of solution C was added to 1 mL of the supernatant. This mixture boiled for 20 min and cooled down in a cold-water bath for 5 min. Next, 1 mL arsenomolybdate solution added to the mixture. This tube was stirred for a short period and warmed at 37 °C for 5 min. The solution was diluted with 5 mL distilled water, stirred and the absorbance was measured at λ_{max} 745 nm.

RESULTS AND DISCUSSION

FT-IR: Fig. 1 shows the FTIR spectrum of synthetic humin. The broad absorption band observed at around 3426 $cm^{-1}$was due to the O-H stretching vibration of the phenol from hidrochar and carboxylic acid group of biochar. This band may be overlap with N-H stretching vibration band from peptide linkage [9] because the band of O-H group shifted to the higher wavenumber from 3400 cm^{-1}. The high intensity and broad-band indicated hydrogen bondings between O-H and N-H group in sample.

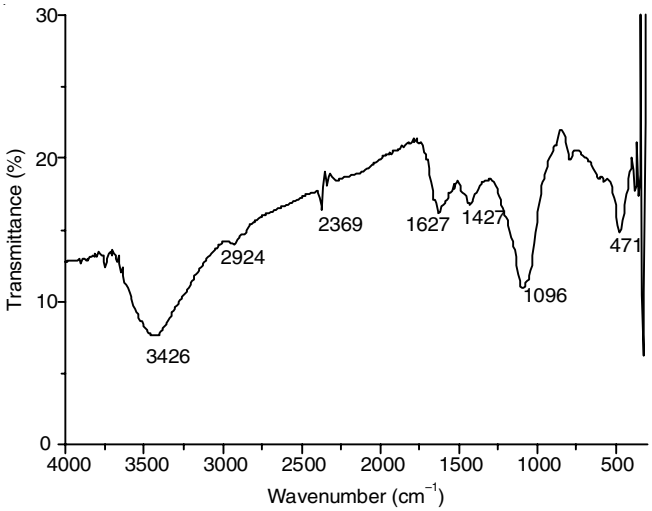

Fig. 1. IR spectra of synthetic humin

The peaks at 2924 and 1427 cm^{-1} were assigned to the C-H stretching and bending vibration of alkyl group [10]. These band was also assigned to CH_3-Si bond [11] from the silicate component of biocharon synthetic humin. The sharp band at 1096 cm^{-1} was ascribed to C-O stretching vibration of alcohol or phenol on hidrochar structure and to the Si-O asymmetrical stretching vibration of the silicate component [12]. The finger print band of silicate presence on humin synthetic shown by 471 cm^{-1} sharp band was assigned to Si-O-R (R=Al, Fe) asymmetrical bending vibration [12]. The aromatic component shown at 1627 cm^{-1} was due to C=C aromatic group of biochar. The band near 1600 cm^{-1} is a relative pure ring stretching mode strongly associated with the aromatic C–O–CH_3 stretching mode [13].

Humin is a partial supramolecular composition of trapped aliphatic hydrocarbons, proteins, carbohydrates, covalently-bond fatty acids and trapped fatty acids and/or esters [6]. Supramolecular compound forms by hydrogen bond, van der Waals forces and/or other weak intermolecular forces [5]. The presence of these band were shown by broad band at 3650-3600 cm^{-1}, which indicated hydrogen bonds between N-H and/or O-H groups from hidrochar and biochar in synthetic humin.

X-ray diffraction: X-ray diffractogram of synthetic humin (Fig. 2) clearly shown that the nature of synthetic humin is

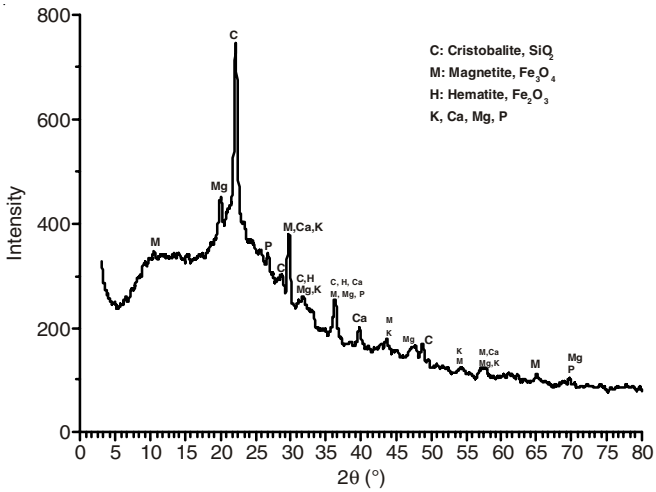

Fig. 2. Diffractrogram of synthetic humin

amorphous carbon of cellulose [14] as matrix sample from biochar and reinforced by the symmetric peak at 4.00939 Å. The inorganic component of synthetic humin was dominated by cristobalite, the amorphous quartz group (SiO_2) from biochar as shown by the sharp and strong peak at *d*-spacing 4.00939 Å [15]. The mineral cristobalite is a high-temperature polymorph of silica, meaning that it has the same chemical formula, SiO_2, but a distinct crystal structure. Both quartz and cristobalite are polymorphs with all the members of the quartz group, which also include coesite, tridymite and stishovite. Presence SiO_2 showed by peaks about 3.13, 2.8, 2.47 and 1.86 Å [16,17]. Besides SiO_2, there are several inorganics component on synthetic humin such as K, Ca, P and Mg as nutrient for plant growth and indicated fertility of soil. The peaks at 3.005, 2.8 and 1.6 Å were assigned to K as a single atom. The peaks at 3.005, 2.47, 2.26 and 1.6 were indicate to Ca atom in $CaCO_3$ molecule [18-20]. The peaks around 3.321, 2.47 and 1.3 assigned to P was mainly associated with particulate solids [18] and 4.43, 2.8, 2.47, 1.8, 1.6 and 1.3 Å were Mg patterns as MgO molecule [21]. Presence of Fe on synthetic humin forms both of Fe_2O_3 and Fe_3O_4 based on diffractogram. Atom Fe in form Fe_2O_3 have peaks at 2.8 and 2.47 Å [22-24] and at 8.46, 3.005, 2.47, 2.07, 1.6 and 1.4 indicated Fe_3O_4 [24,25].

Surface area analysis (BET analysis): The result of surface area analysis of synthetic humin by BET method showed that the average specific surface area of synthetic humin was 40.408 $m^2 g^{-1}$ and total pore volume of synthetic humin was 0.08429 cc g^{-1} with average pore diameter was 8.8434 nm. The total pore volume was determined from the amount of nitrogen adsorbed at a relative pressure close to unity assuming that all the pores were filled with nitrogen at the particular pressure [26]. The BET constant, C was 38.081, reflects the difference in the energy of adsorption for the first layer compared to the difference in adsorption of subsequent layers on top of those already adsorbed. Fig. 3 shows the adsorption/desorption isotherm nitrogen at 77.3 K. The graph was type IV with H3 loop hysteresis as IUPAC classification of the sorption isotherm [27].

The type IV adsorption isotherm is typical for mesoporous adsorbents, proved by calculation of average pore diameter synthetic humin was around 8.8434 nm where material with diameter pore 2-50 is mesoporous materials [27]. At higher pressures, the slope shows increased uptake of adsorbate as a pores filled, inflection point typically occurs near completion of the first monolayer (B point). Adsorption at monolayer was reversible but irreversible at multilayer, showed at graph Fig. 3. There was loop hysteresis occurred after B point showed that amount of gas molecule desorbed was not equaled with adsorbed. Loop hysteresis is type H3 indicates there is pore network inside material [27]. In this material, the distribution of pore sizes and the pore shape is not well-defined because the pore size distribution was not spread evenly. A sharp step on the desorption isotherm usually a sign of interconnection of the pores and if a pore connected to the external phase *via* a smaller pore, in many cases the smaller pore acts as a neck form an ink-bottle pore.

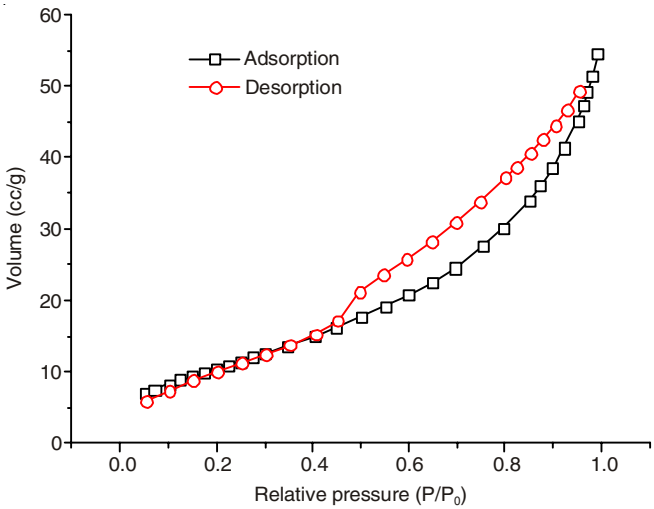

Fig. 3. Adsorption-desorption isotherm of synthetic humin

Adsorption study

Effect of pH: The pH of glucose solution was varied between 4 to 9 to mimic the natural pH condition of soils. Fig. 4 shows the influence of pH on the glucose adsorption on synthetic humin. There was no significant change of adsorption capacity value in all pH condition, which meant pH was not affecting the glucose adsorption on synthetic humin. This proved that the humin as the most stabile fraction of humic substances, was not dilute and changed in all pH condition [6]. Hence, pH of the solutions was adjusted unintentionally during the entire experiment.

Effect of initial concentration: The effect of initial glucose uptake on synthetic humin was examined at five concentration level range from 10 to 300 mg L^{-1} (Fig. 5). Adsorption increased with increasing concentration of glucose solution. The larger number of molecule completely occupied the active sites of the surface of the adsorbent, which was not occurred in a lower concentration. That was cause inconsistently increasing adsorption capacity in lower concentration. After 100 mg L^{-1}, amount of glucose molecule quite a lot to cover active sites of adsorbent, the graph of adsorption capacity increase consistently.

Effect of contact time: The adsorption capacity of glucose increased with increasing contact time until reach equilibrium. At the first 24 h occurred glucose adsorption and

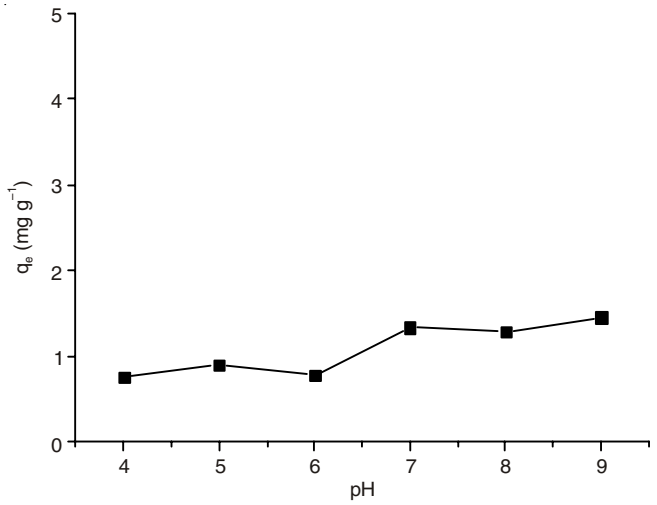

Fig. 4. Effect of pH glucose solution on synthetic humin (w = 0.5 g, time = 2 h, V adsorbate = 25 mL, $C_{glucose}$ = 100 mg L^{-1}, T = ambient temperature)

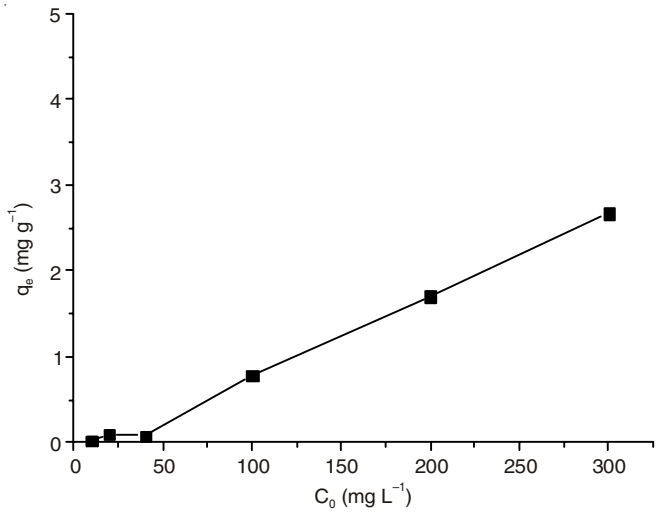

Fig. 5. Effect of initial glucose concetration on synthetic humin (w = 0.5 g, time = 2 and 24 h, V adsorbate = 25 mL, pH = 6, T = ambient temperature)

rate increase significant in 48 h. After that, the rate of glucose uptake decreases sharply. Adsorption analyzed after equilibrium until a month or 720 h to ensure that the equilibrium data are indeed at equilibrium (Fig. 6). Lower glucose concentration in the solid phase at low solute concentration, indicated that adsorbate-adsorbate interactions are stronger that adsorbate-adsorbent interactions [28] caused need longer time to reach equilibrium than metal or dyes adsorption by humin [29]. Firstly, glucose-water interaction was strong enough, each glucose hydroxyl group forms two hydrogen bonds to water [30]. Energy and longer time needed to break glucose-humin interaction. Molecule collision slowly could make that interaction break and started to form glucose-humin interaction. Good contact between the solid adsorbent and the liquid phase is crucial for reaching adsorption equilibrium [31].

Adsorption kinetics

Pseudo first order model of Lagergern [32]:

$$\log (q_e - q_t) = \log q_e - \frac{k_1}{2.303} t \quad (2)$$

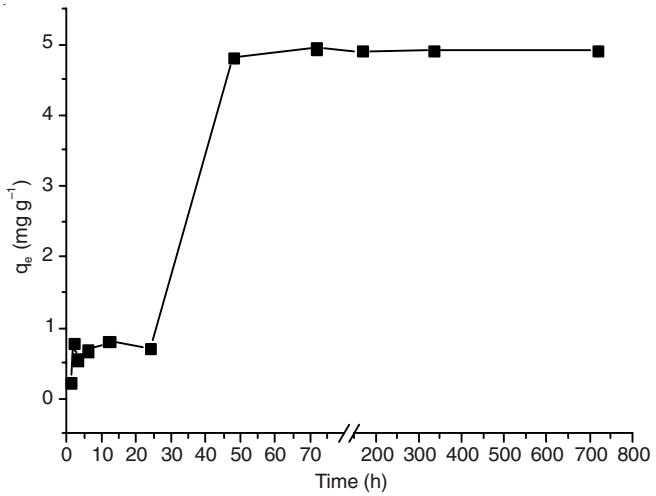

Fig. 6. Effect of contact time adsorption glucose on synthetic humin (w = 0.5 g, V adsorbate = 25 mL, $C_{glucose}$ = 100 mg L^{-1}, pH = 6, T = ambient temperature)

where q_e (mg g^{-1}) is the amount of adsorbate adsorbed at equilibrium and q_t (mg g^{-1}) is the amount of adsorbate on the surface of adsorbent at any time, t. k_1 is the rate constant of pseudo first order adsorption (min^{-1}) which can obtained from the slope of the plot log (q_e-q_t) *vs*. t.

Pseudo order 2 Ho and McKay [33] (Fig. 7):

$$\frac{t}{q_t} = \frac{1}{k_2 q_e^2} + \frac{t}{q_e} \quad (3)$$

where k is the rate constant of pseudo second order adsorption (g mg^{-1} min^{-1}), q_e (mg g^{-1}) is the amount of adsorbate adsorbed at equilibrium and q_t (mg g^{-1}) is the amount of adsorbate on the surface of adsorbent at any time, t.

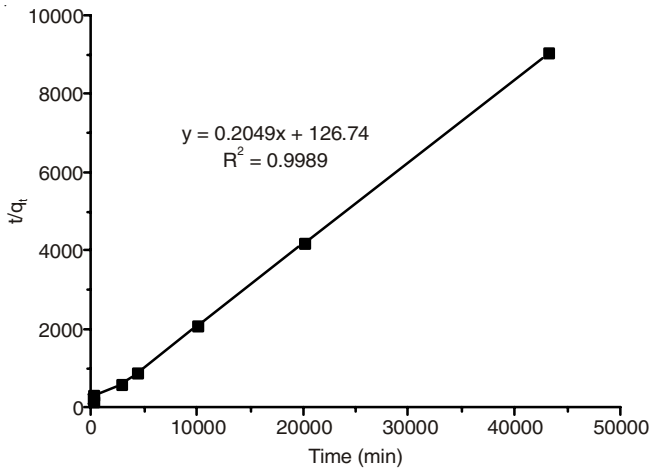

Fig. 7. Adsorption kinetic pseudo second order model of Ho & McKay [33]

Table-1 showed that the resulting pseudo second order model has the highest level of linearity then pseudo first order model with R^2 value is 0.9647. Rate constant of adsorption is 8.42×10^{-5} g mg^{-1} min^{-1}. This model describes reaction rate is dependent on the quantity of solute adsorbed in the surface of the adsorbent and on the quantity adsorbed at equilibrium [33]. Value of q_e is quite similar between q_e calculation is 5.26 and q_e experiment is 4.813 mg g^1 which means every a gram adsorben about 5 mg adsorbate would be adsorbed.

TABLE-1
COMPARISON OF PSEUDO FIRST AND PSEUDO SECOND ORDER MODELS FOR GLUCOSE ADSORPTION ON SYNTHETIC HUMIN

Kinetics model	Rate constant, k	R^2	q_e (mg g^{-1})	q_e experiment
Pseudo first order of Lagergren	1×10^{-4} min^{-1}	0.5043	1.1872	4.813
Pseudo second order of Ho	$8{,}42 \times 10^{-5}$ g mg^{-1} min^{-1}	0.9647	5.2600	

Adsorption isotherm: To establish the most appropriate correlation from the result at equilibrium, to understand how the glucose adsorbed by adsorbent and to calculate the maximum adsorption capacity, adsorption isotherm were studied. There are various adsorption isotherm models, Langmuir and Freundlich are two models and McKay which are most commonly used for adsorption isotherm studies. Linear regression used to determine the best fitting model.

Langmuir model is the simplest and the most widely used sorption isotherm, adsorption occurs uniformly on the active sites of monolayer adsorbent surface. Monolayer means that once an adsorbate occupies an active site, no further adsorption can take place that site. The Langmuir equation is:

$$\frac{C_e}{q_e} = \frac{1}{q_0 K_l} + \frac{C_e}{q_0} \quad (4)$$

where q_e is the amount of glucose adsorbed at equilibrium (mg g^{-1}), C_e is the equilibrium solution concentration (mg L^{-1}), q_0 and K_l are the Langmuir constants represent the maximum adsorption capacity (mg g^{-1}) and energy of adsorption, respectively. Fitting this model with plot data to C_e/q_e *vs.* C_e should be a straight line with slope $1/q_0$ and intercept $1/q_0 K_l$.

The Freundlich equation is an empirical model applicable to mono or multi-layer adsorption on a heterogeneous surface. This model expressed by the following equation:

$$\log q_e = \log K_f + \frac{1}{n} \log C_e \quad (5)$$

where q_e is the amount of glucose adsorbed at equilibrium (mg g^{-1}), C_e is the equilibrium solution concentration (mg L^{-1}), K_f is the Freundlich constants which represent adsorption capacity and n is adsorption intensity. K_f and n calculated from equation from graph log q_e *vs*. log C_e with slope 1/n and intercept log K_f. The value on n indicates heterogeneous level surface area of adsorbent. Completely, Freundlich models explain that on heterogeneous surface area of adsorbent forming multilayer adsorbate. Adsorbate molecule can moving between parts of surface adsorbent that only several active sites can adsorbed molecule. Interaction between adsorbate and adsorbent active site only invoked by intramolecular interaction such as van der Waals interaction or hydrogen bonding.

Adsorption isothermally fit at high adsorbate concentration, at lower concentration of adsorbate, occur nonlinear graph and there is none model fitting with data. When glucose activity on solution higher than on surface adsorbent, adsorption isotherm start to form linear graph. It might be because at lower glucose concentration, adsorbate-adsorbate interactions are stronger than adsorbate-adsorbent interactions. Based on R^2 value on Table-2, the data fitted with Freundlich isotherm that explained the multilayer adsorption on synthetic humin, with K_f values was 4.78×10^{-3} mg g^{-1} and n values was 0.870. In Freundlich equation, n values less than 1 showed that adsorbent surface area was heterogen, closer to zero n values, more heterogen surface area that are adsorbed.

TABLE-2
COMPARISON OF LANGMUIR AND FREUNDLICH ISOTHERM MODELS FOR GLUCOSE ADSORPTION ON SYNTHETIC HUMIN

Langmuir		
q_0 (mg g^{-1})	K_L (L mg^{-1})	R^2
10.188	8.506×10^{-4}	0.96087
Freundlich		
n	K_f (mg g^{-1})	R^2
0.870	4.78×10^{-3}	0.99998

Desorption study: Desorption experiment was studied exactly in the same condition with adsorption without adsorbate in solution, only distillated water. The aim of this study to explore the desorbtion of glucose to distilled water spontaneously without microbiological role in modelling natural soil condition. The result was there is no glucose desorbed to distillated water, so we have conclusion that glucose trapped tightly on porous of synthetic humin and it could not be detached without microbiological soil roles. Besides that, a good humin has resistance to microbiological activity, if glucose activities on solution system still enough for plant needed growth, microbiological would not break the macromolecule substances which trapped on humus.

Conclusion

Synthetic humin is a good host for glucose. The 100 ppm initial concentration of glucose can adsorbed by synthetic humin and reach equilibrium at 48 h. The adsorption data were best fitted with Freundlich isotherm model with K values was 0.00478 mg g^{-1}. Glucose adsorption on humin followed pseudo second order kinetics models of Ho's. The adsorption capacity of humin was 4.8 mg g^{-1} with rate constants 8.42×10^{-5} g mg^{-1} min^{-1}. These result proved that synthetic humin as the stable fraction of humus has ability to trap carbon from free macromolecule in solution system.

ACKNOWLEDGEMENTS

The authors thank to Directorate General of Higher Education, Republic of Indonesia, for financial support through BPPDN 2013 Program.

REFERENCES

1. W.R. Howarth, Western Nutrient Management Conference, Vol. 6, pp. 244-249 (2005).
2. E.A. Paul and F.E. Clark, Soil Microbiology and Biochemistry, edn 2, Academic Press, San Diego, Califorina (1996).
3. E.H. Novotny, M.H.B. Hayes, B.E. Madari, T.J. Bonagamba, E.R. Azevedo, A.A. Souza, G. Song, C.M. Nogueira and A.S. Mangrich, *J. Braz. Chem. Soc.*, **20**, 1003 (2009).
4. M.H.B. Hayes, R.S. Swift, C.M. Byrne, G. Song and A.J. Simpson, International Humic Substances Society (IHSS) (2010).
5. A. Piccolo, *Adv. Agron.*, **75**, 57 (2002).
6. G. Song, E.H. Novotny, A.J. Simpson, C.E. Clapp and M.H.B. Hayes, *Eur. J. Soil Sci.*, **59**, 505 (2008).

7. D. Smejkalová and A. Piccolo, *Environ. Sci. Technol.*, **42**, 699 (2008).
8. IHSS, Carbohydrates Compositions of IHSS Samples (2010).
9. J. Kong and S. Yu, *Acta Biochim. Biophys. Sin.*, **39**, 549 (2007).
10. C.H. Chia, B. Gong, S.D. Joseph, C.E. Marjo, P. Munroe and A.M. Rich, *Vib. Spectrosc.*, **62**, 248 (2012).
11. A. Naidja, P.M. Huang, D.W. Anderson and C. dan Van Kessel, *Appl. Spectrosc*., **56**, 318 (2002).
12. B.J. Saikia, G. Parthasarathy and N.C. Sarmah, *Bull. Mater. Sci.*, **31**, 775 (2008).
13. R. Bodirlau and C.A. Teaca, *Rom. J. Physiol.*, **54**, 93 (2009).
14. D. Ciolacu, F. Ciolacu and V.I. Popa, *Cellul. Chem. Technol.*, **45**, 13 (2010).
15. H. Yilmaz and H. Kacmaz, *Appl. Clay Sci.*, **62-63**, 80 (2012).
16. S.V. Vassilev, D. Baxter, L.K. Andersen, C.G. Vassileva and T.J. Morgan, *Fuel*, **94**, 1 (2012).
17. P. Yu, Y. Tsai, F.-S. Yen, W.-P. Yang and C.-L. Huang, *J. Eur. Ceram. Soc.*, **35**, 673 (2015).
18. K. Güngör, A. Jürgensen and K.G. Karthikeyan, *J. Environ. Qual.*, **36**, 1856 (2007).
19. Y. Ma, Q. Wang, X. Sun and X. Wang, *Biomass Conv. Bioref*., **5**, 339 (2014).
20. S. Ramola, T. Mishra, G. Rana and R.K. Srivastava, *Environ. Monit. Assess.*, **186**, 9023 (2014).
21. M. Song, M. Chen and Z. Zhang, *Mater. Charact.*, **59**, 514 (2008).
22. S.K. Sahoo, K. Agarwal, A.K. Singh, B.G. Polke and K.C. Raha, *Int. J. Eng. Sci. Technol.*, **2**, 118 (2010).
23. M.R. Joya, J.B. Jaimez and J.B. Ortega, *J. Phys.; Conference Series*, **466**, 012023 (2013).
24. N. Du, Y. Xu, H. Zhang, C. Zhai and D. Yang, *Nano. Res. Lett.*, **5**, 1295 (2010).
25. H.E. Ghandoor, H.M. Zidan, M.M.H. Khalil and M. Ismail, *Int. J. Electrochem. Sci.*, **7**, 5734 (2012).
26. M. Goswami, L. Borah, D. Mahanta and P. Phukan, *J. Porous Matter.*, **21**, 1025 (2014).
27. IUPAC, *Pure Appl. Chem.*, **57**, 603 (1985).
28. O.D. Nartey and B. Zhao, *Adv. Mater. Sci. Eng*., Article ID 715398 (2014).
29. M. Francisco, A.N. Mlinar, B. Yoo, A.T. Bell and J.M. Prausnitz, *Chem. Eng. J.*, **172**, 184 (2011).
30. A.M.D. Jesus, L.P.C. Romão, B.R. Araújo, A.S. Costa and J.J. Marques, *Desalination*, **274**, 13 (2011).
31. M. Antonietti, Department of Colloid Chemistry, Max Planck Institute of Colloids and Interface, Postdam Personal Communication, pp. 12-22 (2006).
32. S. Lagergren, *Vetenskapsakad. Handl.*, **24**, 1 (1898).
33. Y.S. Ho and G. McKay, *Process Biochem.*, **34**, 451 (1999).
34. P. Bai, J.I. Siepmann and M.W. Deem, *AlChE J.*, **59**, 3526 (2013).